Energy Storage Materials 16 (2019) 505–511

Contents lists available at ScienceDirect

Energy Storage Materials

journal homepage: www.elsevier.com/locate/ensm

# A scalable 3D lithium metal anode

Haodong Liu, Xiujun Yue, Xing Xing, Qizhang Yan, Jason Huang, Victoria Petrova, Hongyao Zhou, Ping Liu*

*Department of NanoEngineering, University of California San Diego, La Jolla, CA 92093, USA*

ARTICLE INFO

*Keywords:*
Li metal anode
Dendrite Free
High coulombic efficiency
Porous host
3D host

ABSTRACT

A scalable 3D electrode to serve as a lithium metal host is developed to enable stable lithium metal cycling. The electrode is simply fabricated by coating a slurry of well mixed $LiNO_3$, carbon black, and PVDF on the Cu foil. The pores in the electrode serve as lithium metal hosts while the $LiNO_3$ particles act both as a structural skeleton and an electrolyte additive. Micron-level dense Li chunks are deposited into the 3D electrode at a current density of 2 mA $cm^{-2}$. Moreover, high coulombic efficiencies of 98.4% and 97.1% are achieved in carbonate-based electrolytes at current densities of 0.25 mA $cm^{-2}$ and 2 mA $cm^{-2}$, respectively. The 3D electrode is tested in an anode free cell with $LiFePO_4$, which exhibits a good capacity retention of 49.1% after 100 cycles and correspond to an average efficiency of 99.3% per cycle. This work provides a facile and scalable method to fabricate multi-functional 3D electrodes for dendrite-free and high coulombic efficiency Li metal anodes.

## 1. Introduction

Li metal anode is currently being extensively studied to replace graphite in order to further raise the energy density of rechargeable batteries [1]. Li metal anode, however, has been plagued by several well-known issues. Dendritic Li formation during repeated Li plating and stripping results in ever increasing surface area and may short the cell over time and cause safety issues. The loose deposition of Li anode also results in large volume expansion [2–5]. Perhaps the most challenging is the low coulombic efficiency (CE). The continuous loss of active lithium does not satisfy the requirement of long cycling life when limited Li is used in order to achieve high energy density. These challenges have been well reviewed recently. The root causes of these problems are the high reactivity of Li metal and non-uniform Li ion flux [1].

Several approaches have been presented recently to address these challenges [6–12]. In order to mitigate the lithium metal reaction with the electrolyte, research has identified ether based electrolytes to be more stable than carbonate based ones, resulting in higher coulombic efficiency. Unfortunately, these electrolytes have poor oxidative stability and are usually unsuitable for high voltage, oxide based cathodes [13–15]. Another widely used method is to employ electrolytes (often with additives) that promote the formation of high quality solid electrolyte interface (SEI) formation to protect lithium metal. This method is applicable to the more oxidatively stable, carbonate-based cathodes. For example, Xu simultaneously added $LiAsF_6$ and cyclic carbonate into the electrolyte to generate a uniform and flexible SEI layer on the Li surface, which contributes to dendrite free Li deposition with enhanced coulombic efficiency [16]. In order to address the large volume changes during Li plating and stripping, other researchers have introduced 3D hosts for Li metal, such as porous Cu, layered reduced graphene oxide, and carbon cloths, among others [17–19]. These 3D hosts not only largely mitigate the volume changes during Li plating and stripping, but also suppress the Li dendrite growth. Although, the large surface area of the 3D host reduces the local current densities, the side reactions become more serious as well. An effective strategy would therefore require combining 3D host design with electrolyte engineering to address all the issues of the Li metal anode.

In this work, a commercial carbonate electrolyte (1 M $LiPF_6$ in 1:1 vol ratio EC/DMC, LP30) is chosen as the baseline. By adding vinylene carbonate and $LiNO_3$, both Li metal morphology and coulombic efficiency are greatly improved. Later, this modified electrolyte is combined with a novel multi-functional 3D composite host for the Li metal anode. As shown in Scheme 1**a**, this 3D composite host is prepared by simply casting a well mixed slurry of $LiNO_3$, carbon black, and PVDF on a Cu foil, followed by drying in the oven. As a result of the combination of electrolyte additive and 3D composite host, dense Li chunks with micron-sized particles are observed even at a high current density of 2 mA $cm^{-2}$ after 70 cycles in a carbonate electrolyte. A high coulombic efficiency of 98.4% over 300 cycles has also been achieved at

* Corresponding author.
*E-mail address:* piliu@eng.ucsd.edu (P. Liu).

https://doi.org/10.1016/j.ensm.2018.09.021
Received 11 July 2018; Received in revised form 10 September 2018; Accepted 25 September 2018
Available online 26 September 2018

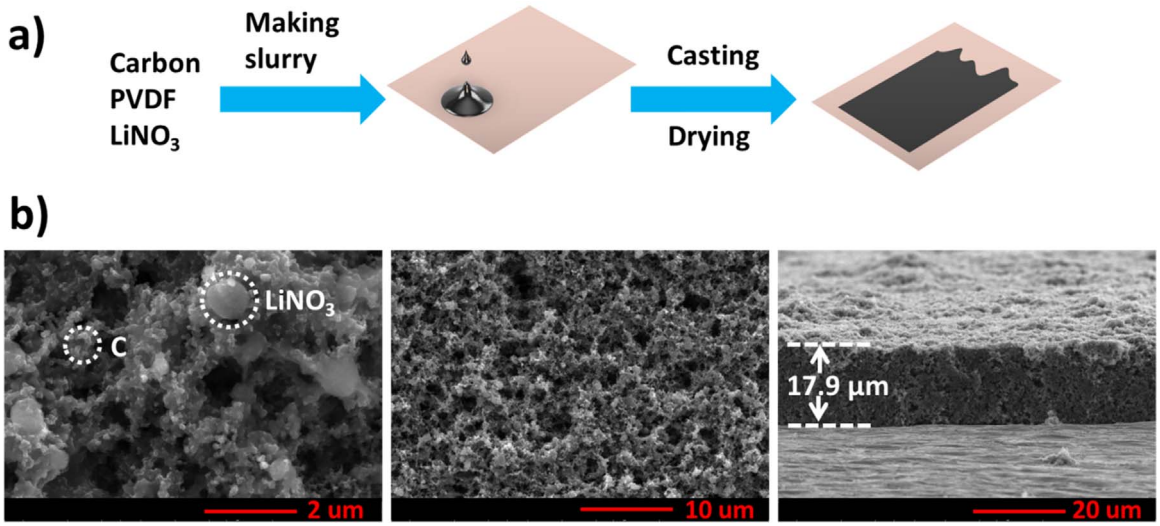


**Scheme 1. a)** The process of making the 3D composite host; b) SEM images of the 3D $LiNO_3$ composite host.

0.25 mA $cm^{-2}$ for 0.5 mAh $cm^{-2}$. This work suggests that simultaneous use of electrolyte additives and 3D hosts are necessary to enable stable Li metal anode.

## 2. Experimental method

### 2.1. 3D composite electrode preparation

The 3D composite electrode was prepared by mixing the $LiNO_3$ (Sigma-Aldrich), with 20 wt % Super P carbon (TIMCAL) and 20 wt % poly(vinylidene fluoride) (PVDF) in N-methylpyrrolidone (NMP, ACROS Organics). The slurry was cast onto a Cu foil using a doctor blade and dried in a vacuum oven overnight at 80 °C. The electrode discs were punched and dried again before being storing in an argon-filled glovebox (MTI corporation).

### 2.2. Electrochemical test

Battery grade vinylene carbonate (VC) was acquired from Shenzhen CAPCHEM Technology Co. Ltd. The premixed LP30 electrolyte (1 M $LiPF_6$ in 1:1 vol ratio EC/DMC) was purchased from BASF.

2032-type coin cells were used for all the electrochemical studies in this work. The 250 µm thick lithium was punched to 12.5 mm discs as the counter electrode. The Celgard 25 µm trilayer PP-PE-PP membrane was used as a separator. Galvanostatic cycling was conducted on an LBT-5V5A battery tester (Arbin instruments). The cycled electrode was recovered by disassembling the coin cell. All the samples were washed with DMC three times and dried in the glovebox antechamber under vacuum.

### 2.3. Scanning electron microscopy

The morphology and thickness of the deposited Li metal film and 3D composite electrode were characterized using scanning electron microscopy (FEI Quanta 250 SEM). The sample was adhered to a double-sided carbon tape and placed on a specimen holder. The prepared sample was sealed in a laminate plastic bag inside the glovebox for transferring to the SEM. The approximate time of sample exposed to air (from a sealed environment to the SEM stage) was less than 3 s.

### 2.4. X-ray diffraction

The crystal structure of coating materials were identified by X-ray diffraction (XRD), acquired using a Bruker D2 phaser diffractometer with a Bragg- Brentano θ-2θ geometry and a Cu Kα source (λ = 1.54 Å). Samples were sealed inside the glovebox by kapton tape, which were scanned from 30° to 60° at a scan rate of 0.02° $s^{-1}$.

## 3. Results and discussion

The coulombic efficiency of Li metal cycling depends on the electrolyte solvent. Due to its high compatibility with oxide based cathodes, it is critical to enhance the Li stability in carbonate based electrolytes. A commercial electrolyte (1 M $LiPF_6$ in 1:1 vol ratio EC/DMC, LP30) was chosen as a baseline electrolyte in this work. Based on previous Si anode research, 5 wt% vinylene carbonate (VC) was chosen as an SEI formation additive in order to improve the uniformity and flexibility of the SEI film on Li surface [16]. The effects of VC additive on Li metal CE were studied by testing Li–Cu coin cells. Li was plated on Cu substrate at 0.5 mA $cm^{-2}$ for 1 mAh $cm^{-2}$, and then stripped at the same current density until the cell potential reached 1 V. The results of LP30 electrolyte (E1) and LP30 + 5 wt% VC electrolyte (E2) are compared in Fig. S1. The average CE over 80 cycles is improved from 90.5% to 96.9% with the help of the VC additive.

Our second additive is $LiNO_3$. Previous work has shown that $LiNO_3$ is a universal electrolyte additive in Li-S batteries because it protects the Li metal and reduces the $S_n^{2-}$ shuttle by forming a layer of $Li_xNO_y$ species [20,21]. The concentration of the $LiNO_3$ in ether-based electrolytes for Li-S batteries is usually higher than 0.2 M. Because of the low solubility of $LiNO_3$ in carbonates, $LiNO_3$ has not been widely used in carbonate-based electrolytes yet [21]. The $LiNO_3$ salt was gradually added into the E2 until saturation; the overall concentration of $LiNO_3$ was 0.02 M. As shown in Fig. S1, this LP30 + 5 wt% VC + 0.02 M $LiNO_3$ (E3) electrolyte further enhanced the CE of Li metal to 97.7%.

In addition to the CE test, the Li deposition morphologies were also investigated in these electrolytes. Li was plated on the Cu substrate at a high current density of 2 mA $cm^{-2}$ for 1 h. Fig. 1 **and** Fig. S2 present the Li morphologies in these electrolytes. The Li plated in E1 is needle-like. Due to the loose deposition, most mossy Li is lost during cell disassembling. It is hard to determine the thickness of the plated Li in E1 through the cross sectional view. The VC promoted Li chunk formation, however, small amounts of dendrites were also observed in E2 at a high current density of 2 mA $cm^{-2}$. The Li chunk size distribution ranges from 0.5 to 2 µm. The thickness of the Li film in E2 was 26 µm, which suggests that even though the morphology was improved, the deposition is still incompact. According to theoretical calculations, 2 mAh $cm^{-2}$ of Li corresponds to a thickness of 9.7 µm

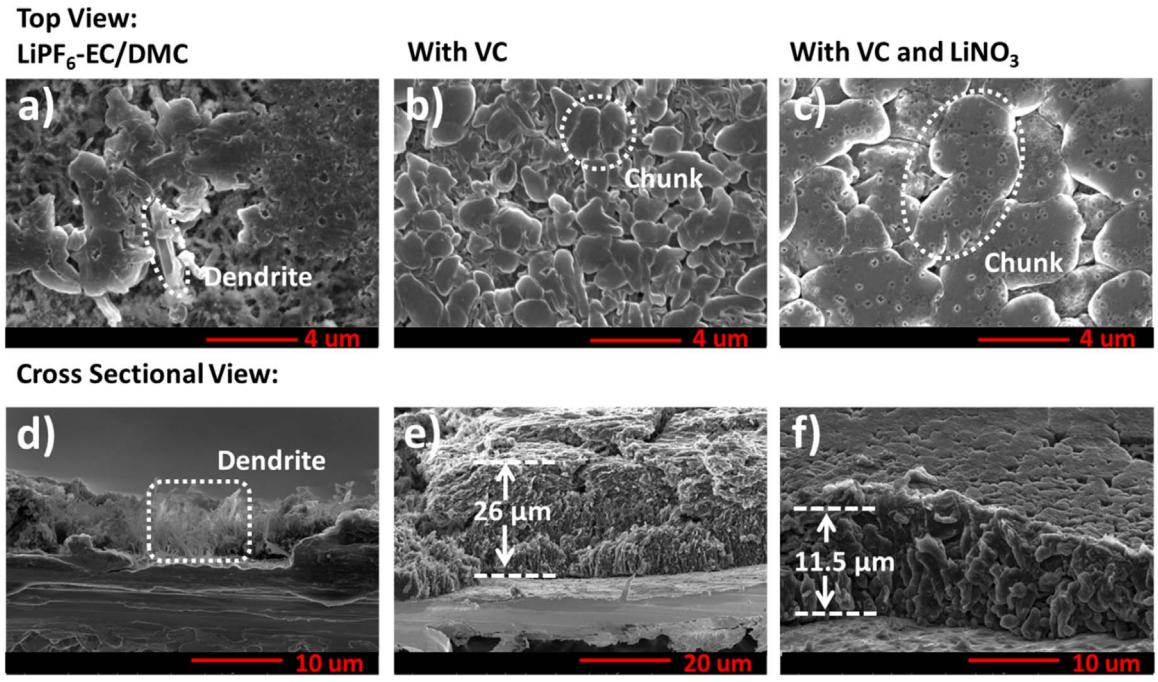


**Fig. 1.** SEM images of the deposited Li metal film on Cu foil. a), b), c) are the top view and d), e), f) are the cross-section view of Cu after 1 hour Li deposition at 2 mA $cm^{-2}$ in 1 M $LiPF_6$-EC/DMC electrolyte (E1), 1 M $LiPF_6$-EC/DMC electrolyte with 5 wt% VC (E2), and 1 M $LiPF_6$ + 0.02 M $LiNO_3$-EC/DMC electrolyte with 5 wt% VC (E3), respectively.

and the porosity of Li in E2 is thus 62.7%. In the case of E3, the plated Li are all big chunks with sizes between 2 and 5 µm. The Li film was 11.5 µm thick with a low porosity of 15.7%, which indicates a dense Li film was deposited on Cu in E3. All the morphology studies of the deposited Li are consistent with the CE testing data. The bigger Li chunk with denser deposition delivers higher CE. The E3 was used as the optimized electrolyte for the rest of the studies.

Although electrolyte formulas are effective in improving cycling efficiency, they don't address the volume change issue during Li cycling. The 3D Li host is a promising strategy. However, the current proposed 3D Li hosts are either too complicated to fabricate, or too hard to implement into a real device [3]. Most of the 3D Li hosts only serve as high surface area porous electrode. Here, a multi-functional 3D composite host was designed. The fabrication of this host is similar to the electrode making process in industry, which is schematically showed in Scheme 1. The SEM images display the porous structure of the host. The porosity of the 3D composite electrode is calculated based on the following equation.

$$\text{Porosity} = \frac{(V_{electrode} - \sum V_{component})}{V_{electrode}} = \frac{V_{electrode} - M_{electrode} \cdot \left(\frac{P_{LN}}{\rho_{LN}} + \frac{P_C}{\rho_C} + \frac{P_{PVDF}}{\rho_{PVDF}}\right)}{V_{electrode}}$$

where $V_{component}$ and $V_{electrode}$ are the components ($LiNO_3$, PVDF, and carbon black) and electrode volume, $M_{electrode}$ is the mass of the electrode, and ρ and P are the density and mass fraction of the materials [22]. The densities of the $LiNO_3$, PVDF and carbon black used for calculating the porosity were 2.38, 1.76, and 2.0 g $cm^{-3}$, respectively. The mass of the electrode is 1.30 mg $cm^{-2}$, and the thickness of the host is 17.9 µm. The calculated porosity of the 3D host is 66.2%. Based on the porosity of the electrode, this 3D host is theoretically able to store 2.44 mAh Li per $cm^2$. Once all the pores are filled by Li, the mass of the deposited Li is calculated to be 0.63 mg $cm^{-2}$, which corresponds to a high gravimetric capacity of 1264 mAh $g^{-1}$.

The performance of the 3D composite host was investigated by the CE test in E3. The bare Cu cycled in E3 was chosen as a baseline. Both bare Cu and 3D composite host were discharged versus Li at 0.5 mA $cm^{-2}$ for 4 h, and then the Li was stripped to 1 V at 0.5 mA $cm^{-2}$ for one cycle. Fig. S3 presents the Li plating and stripping voltage profiles of this conditioning cycle. The purpose of the conditioning cycle is to form an SEI layer on the substrate. The 3D host exhibited a much lower over-potential than the bare Cu, however, the large surface area contributed to the higher irreversibility during this condition cycle. Fig. 2 systematically compared the CE of both substrates at various current densities after their condition cycles. Fig. 2**a** exhibited their CE at 0.25 mA $cm^{-2}$ for 0.5 mAh $cm^{-2}$. At this mild condition, both substrates showed good stability for a long duration of 300 cycles. The 3D host delivered higher average CE than the bare Cu. The average CEs over 300 cycles were 97.5% and 98.4% for bare Cu and 3D host, respectively. Fig. 3 shows the Li plating and stripping voltage profiles on both substrates. The voltage difference between the charge and discharge plateaus was only 37.2 mV on 3D host, while a large voltage difference of 69.1 mV was detected on bare Cu. This lower over-potential was attributed to the porous structure in the 3D host, which decreased the local current density. Both substrates were evaluated at harsher conditions that were closer to the current densities in real batteries. When they were cycled at 1 mA $cm^{-2}$ for 1 mAh $cm^{-2}$, the bare Cu cell started to short before 80 cycles, while the 3D host showed stable Li plating and stripping over 200 cycles. Fig. 2c and Fig. S4 show their CEs and voltage profiles. The bare Cu achieved a CE of only 95.7% for 79 cycles. As a comparison, the 3D host delivered a high CE of 97.9%. The bare Cu cycled at 2 mA $cm^{-2}$ for 2 mAh $cm^{-2}$ presented a much lower cycle life; the Li-Cu cells were usually shorted before 20 cycles. On the other hand, the 3D host still delivered a good CE of 97.1%.

The enhanced CEs were associated with the morphology of the deposited Li. Fig. 4 and Fig. S5 illustrated the Li morphology on the 3D substrate. The first deposition of 2 mAh $cm^{-2}$ Li at 2 mA $cm^{-2}$ showed big chunks of Li similar to the bare Cu substrate. Because the porosity of the 17.9 µm thick 3D host was 66.2%, the pores were able to store 11.8 µm of Li metal. Most of the Li was plated into the 3D host, which filled up all the pores inside the host. As a consequence, the thickness of the Li film was 18.2 µm, which was only 1.7% larger than the original 3D host. Both bare Cu substrate

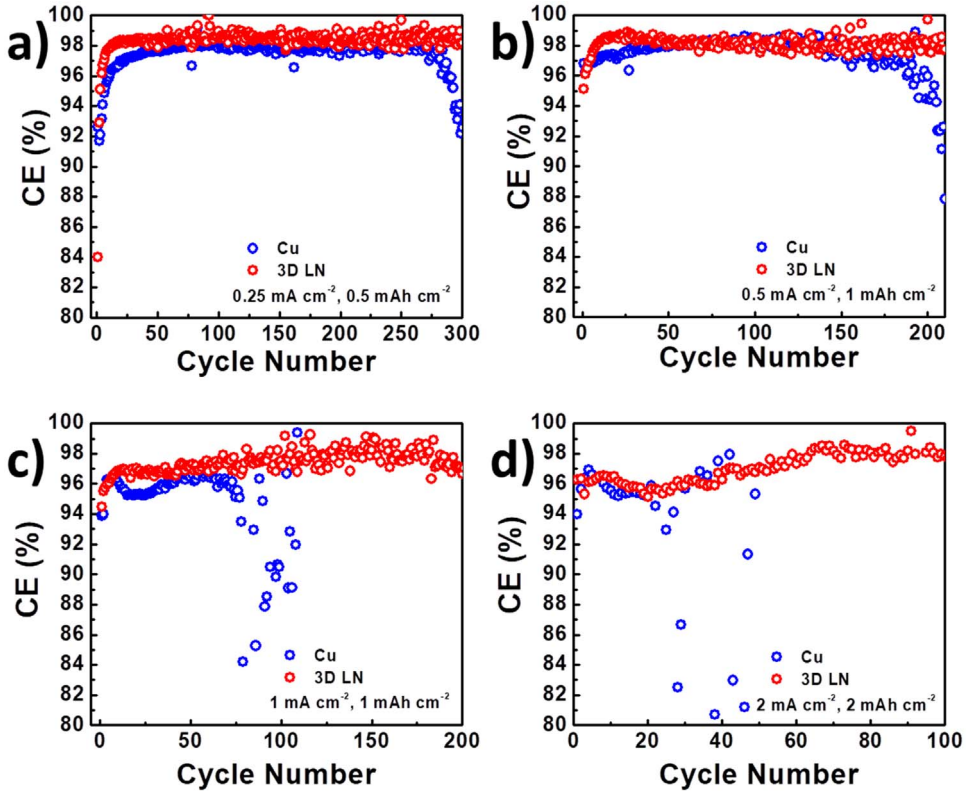


**Fig. 2.** The coulombic efficiency comparison of Li||Cu and Li||3D electrode cells cycled in 1 M $LiPF_6$ + 0.02 M $LiNO_3$-EC/DMC electrolyte with 5 wt% VC, a) at 0.25 mA $cm^{-2}$ for 0.5 mAh $cm^{-2}$; b) at 0.5 mA $cm^{-2}$ for 1 mAh $cm^{-2}$; c) at 1 mA $cm^{-2}$ for 1 mAh $cm^{-2}$; d) at 2 mA $cm^{-2}$ for 2 mAh $cm^{-2}$.

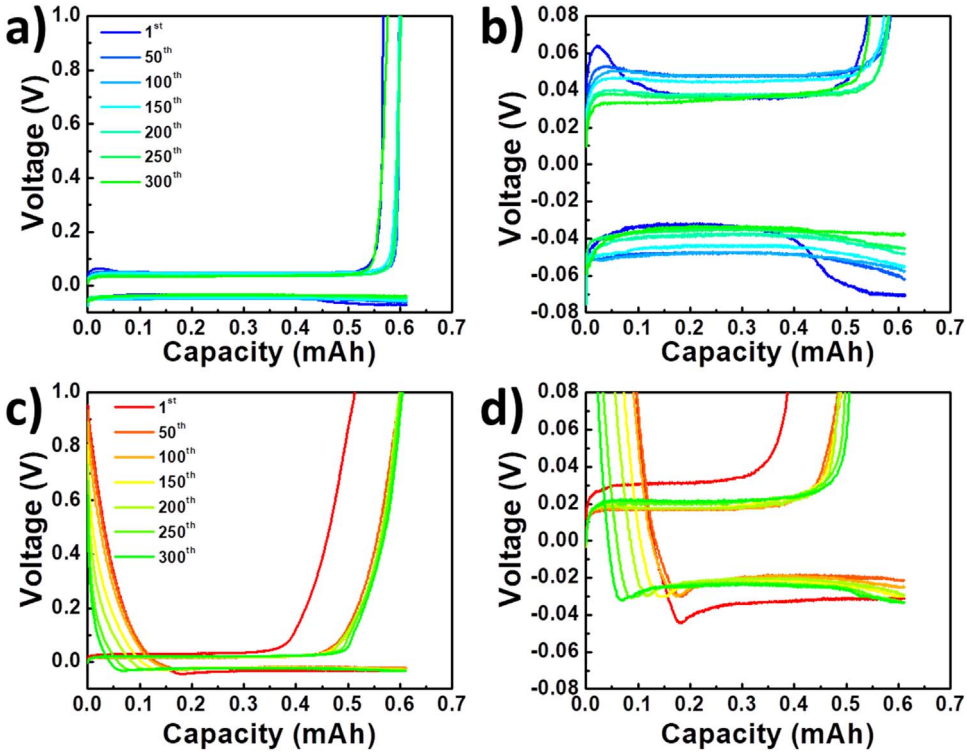


**Fig. 3.** a), and b) the Li plating/stripping voltage profiles on Cu, at 0.25 mA $cm^{-2}$ for 0.5 mAh $cm^{-2}$; c), and d) the Li plating/stripping voltage profiles on 3D $LiNO_3$ composite electrode, at 0.25 mA $cm^{-2}$ for 0.5 mAh $cm^{-2}$.

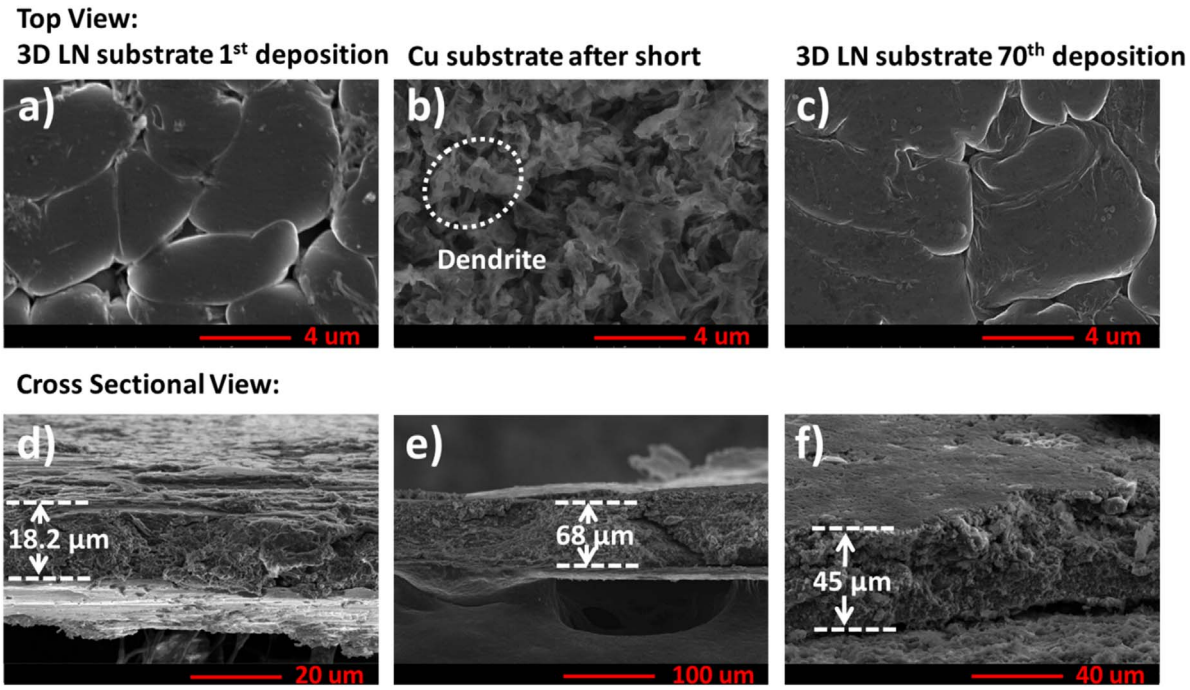


**Fig. 4.** SEM images of the deposited Li metal film in 1 M $LiPF_6$ + 0.02 M $LiNO_3$-EC/DMC electrolyte with 5 wt% VC. a) is the top view and d) is the cross section view of 3D $LiNO_3$ composite electrode after 1 hour Li deposition at 2 mA $cm^{-2}$; b) is the top view and e) is the cross section view of Cu on its 20th deposition; c) is the top view and f) is the cross section view of 3D $LiNO_3$ composite electrode on its 70th deposition; Li depositing at 2 mA $cm^{-2}$ for 2 mAh $cm^{-2}$, then stripping to 1 V at 2 mA $cm^{-2}$.

and 3D composite substrates showed dense Li chunks at the first deposition. However, the cells showed different performances after a few Li plating and stripping cycles at 2 mA $cm^{-2}$ for 2 mAh $cm^{-2}$. Fig. 4b, and e displayed the SEM images of the 20th deposition of the Li on the Cu substrate. All the Li chunks transformed to needles after only 20 cycles, and the thickness of the Li dramatically grew to 68 µm. The short life time of the Li-Cu cell in E3 was caused by the Li dendrite formation as a result of possible $LiNO_3$ depletion. Meanwhile, the morphology of the Li on the 3D composite substrate at its 70th deposition is shown in Fig. 4c, and f**.** The Li chunk morphology was not only well maintained, but also grew larger. Considering the fact that the CE of the 3D host at 2 mA $cm^{-2}$ was less than 100%, there were accumulations of irreversible Li over 70 cycles. Theoretically, if all the deposited Li were 100% dense, the irreversible Li deposition contributed to 23.1 µm increase of the thickness. In reality, the thickness of the Li film increased to 45 µm, which is only 8.9% higher than assuming completely dense depositions (18.2 + 23.1 µm). The investigation on the evolutions of Li morphologies on different substrates verified that the 3D host maintained the dense Li chunks after long term cycling even at high current density.

Anode free cells with $LiFePO_4$ cathode were fabricated to further evaluate the effectiveness of the 3D host. The area capacity loading of the $LiFePO_4$ was 1.5 mAh $cm^{-2}$. Fig. 5 compared the performance of the cells with Cu and 3D host as anode. The cells were cycled between 2.0–4.0 V at 0.5 mA $cm^{-2}$. The 3D host cell showed much higher CEs and better capacity retention than the Cu cell. The Cu cell exhibited an average CE of 97.3% over the course of 50 cycles, which led to a low capacity retention of 25.6% at the 50th cycle. The 3D host cell maintained 49.1% capacity at its 100th cycle with a high average CE of 99.3%. Since an anode free cell does not contain excess lithium, the average CE of the cell was calculated as the $n^{th}$ root of X, where the n is the cycle number and the X is the capacity retention at the $n^{th}$ cycle. Note this efficiency is higher than the average CE of a Li metal cell where Li is only partially cycled. In that case, a fixed amount of Li is cycled during each cycle and CE is averaged over multiple cycles. As far as its performance in Li metal anode batteries with high voltage cathodes, for example, classical layered oxides [23,24], Li-rich layered oxides [25,26], and high voltage spinel [27], we do plan to report the test in our future works as we continue to improve the cycling efficiency.

The importance for both the 3D host structure and abundant $LiNO_3$ reserve is further illustrated with two control experiments. 3D host electrodes without $LiNO_3$ were prepared and compared with the bare Cu and 3D $LiNO_3$ host. The CEs were tested at 0.5 mA $cm^{-2}$ for 1 mAh $cm^{-2}$. The results in Fig. S6 revealed that the 3D porous electrode with only carbon and PVDF could not lead to the superior performance without $LiNO_3$. On the other hand, benefiting from the VC and $LiNO_3$ SEI formation additives, the initial Li deposition on bare Cu was dense and full of chunks. However, due to the low solubility of $LiNO_3$ in the carbonates, it was consumed to passivate the freshly deposited Li surfaces during repeated stripping and plating of Li metal. Once the $LiNO_3$ in the electrolyte was consumed, the dendritic Li started to form. As a comparison, the 3D composite host not only works as a conductive host to mitigate the volume expansion, but also supplies the $LiNO_3$ additive to the electrolyte. In order to prove that the reserved $LiNO_3$ was still maintained inside the 3D host after long term cycling, XRD measurements were performed on both cycled bare Cu and 3D $LiNO_3$ composite host. Fig. 6**a** clearly demonstrated the diffraction peaks of $LiNO_3$ on the 3D $LiNO_3$ composite host even after 70 cycles. A small diffraction peak related to the Li metal was also observed. In contrast to the 3D host electrode, the bare Cu electrode only presented signals from Li metal. XPS characterizations were also conducted on both cycled bare Cu and 3D $LiNO_3$ composite host. Fig. S7 compared the C 1s, O 1s, and N 1s spectra of both electrodes. The C 1s and O 1s spectra revealed that the surface of the 3D $LiNO_3$ composite electrode formed more $Li_2CO_3$ and less Li-alkyl carbonate than the bare Cu. The comparison of the N 1s spectra between both electrodes showed that the $LiNO_3$ reduction compounds $Li_3N$ and $LiN_xO_y$ were formed as SEI components on the surface of the deposited Li film [28]. Moreover, the $Li_3N$ and $LiN_xO_y$ signal on the surface of 3D $LiNO_3$ composite electrode was more prominent, which suggested the 3D $LiNO_3$ composite electrode supplied

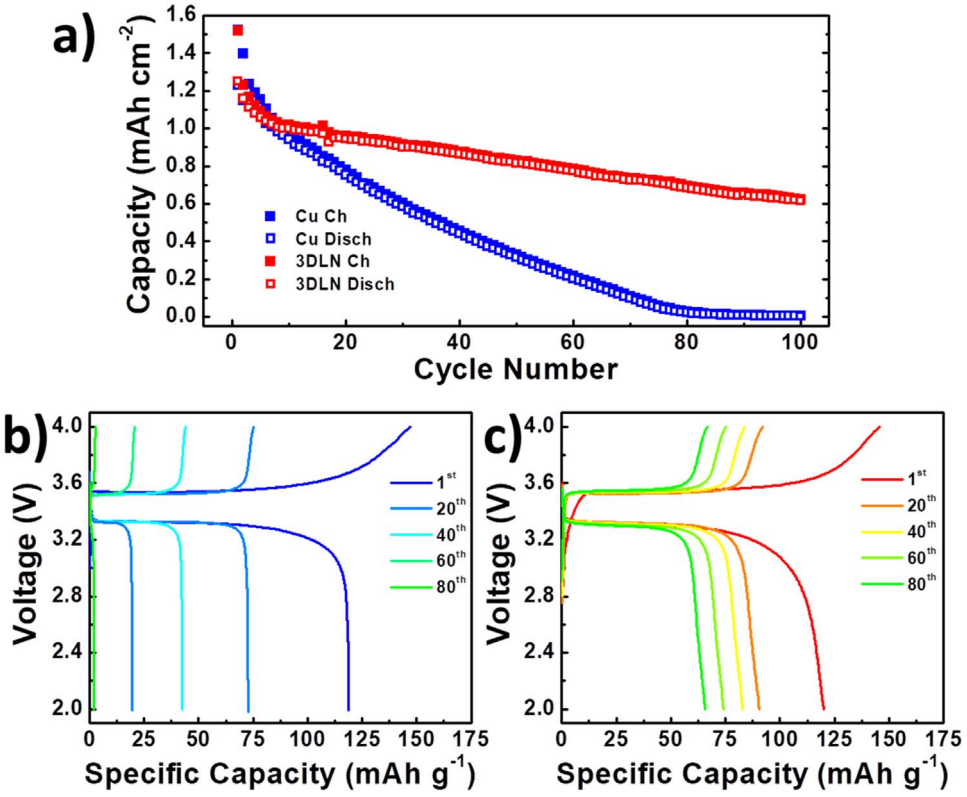


**Fig. 5.** The comparison of anode free full cell performance with $LiFePO_4$ (LFP) as cathode in 1 M $LiPF_6$ + 0.02 M $LiNO_3$-EC/DMC electrolyte with 5 wt% VC. a) is the comparison of capacities and coulombic efficiencies between Cu and 3D $LiNO_3$ composite electrode over the course of 100 cycles; b), and c) are the voltage profiles of Cu-LFP and 3D $LiNO_3$ composite electrode-LFP cells, respectively. The voltage range is 2.0–4.0 V at 0.5 mA $cm^{-2}$.

the $LiNO_3$ additive to the electrolyte. In addition, the $LiNO_3$ peak at 407.4 eV clearly showed the existence of $LiNO_3$ in the 3D composite host after 70 cycles, which is consistent with observations from XRD and SEM. Fig. 6c illustrated that the $LiNO_3$ particles was well retained inside the host after long term cycling. Consequently, big Li chunk morphology with compact depositions was maintained, which led to the high CE.

Scheme 2a illustrates the working mechanism of the 3D composite host. The carbon black in the host provides an electronic conductive network to reduce the local current density and serve as a substrate for Li deposition. The $LiNO_3$ serves as both reserved additive source and a structural skeleton component. The PVDF binder holds all the components together to form the robust porous structure.

To put our results in the context of recently published work, a summary of the Li metal anode coulombic efficiencies in carbonate-based electrolytes was plotted and compared in Scheme 2**b** and Table S1. The CE tests in most of the published literature are conducted at current densities of less than 1 mA $cm^{-2}$ and the Li deposition capacities are lower than 1 mAh $cm^{-2}$. The CEs of Li in the carbonate electrolytes are usually less than 96%. The solid symbols represent the CEs that are achieved in this work. A high CE of 98.4% is reached at a moderate current density of 0.25 mA $cm^{-2}$. At a high current density of 2 mA $cm^{-2}$, the CE remains above 97%.

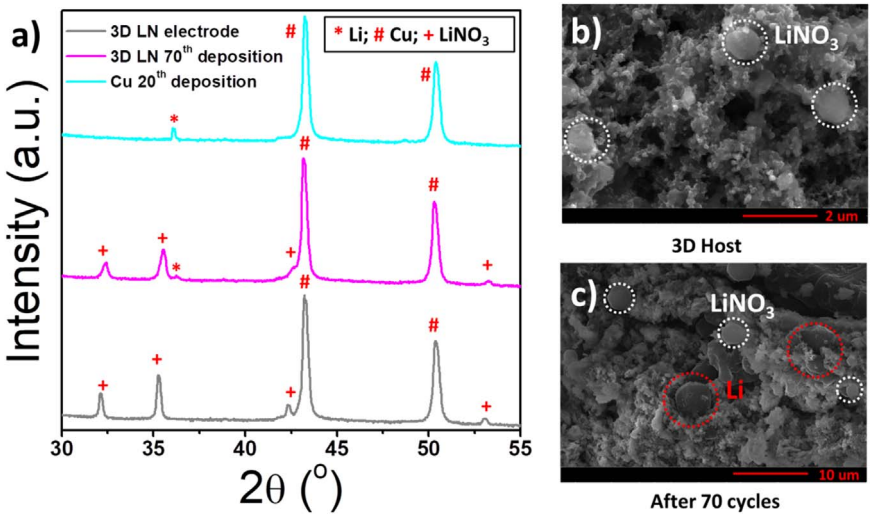


**Fig. 6.** a) XRD patterns. b) – c) SEM images. b) 3D $LiNO_3$ composite host; c) is the cross sectional view of 3D $LiNO_3$ composite electrode on its 70$^{th}$ deposition, Li depositing at 2 mA $cm^{-2}$ for 2 mAh $cm^{-2}$, then stripping to 1 V at 2 mA $cm^{-2}$.

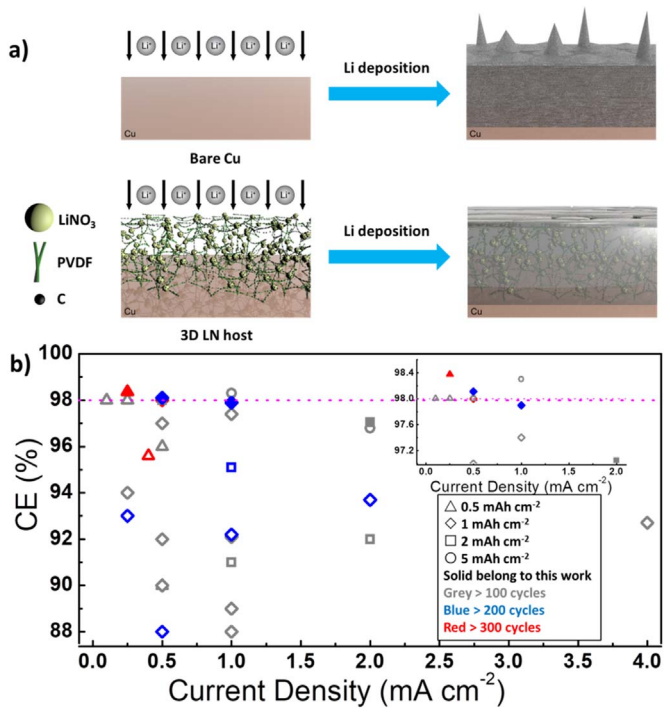


**Scheme 2.** a) The schematic illustration of Li plating/stripping on 3D $LiNO_3$ composite host; b) a summary of the Li metal anode coulombic efficiencies in carbonate based electrolytes.

## 4. Conclusion

In summary, a novel multi-functional 3D composite host is designed for Li metal anode. Due to the robust structure and abundant supplement of the $LiNO_3$, dense Li chunks instead of dendrites are formed and retained after repeated Li plating and stripping at a current density of 2 mA $cm^{-2}$. As a result, the coulombic efficiencies of Li metal on the 3D composite host are reasonably high in the carbonate electrolyte. A high coulombic efficiency of 98.4% has been achieved at 0.25 mA $cm^{-2}$ for a long cycling duration of more than 1200 h. The fabrication process of the 3D host can be easily scaled up by battery manufacturers. This work provides a new route of designing low-cost 3D Li metal for high energy density safe batteries.

## Acknowledgment

This work was supported by the Office of Vehicle Technologies of the U.S. Department of Energy through the Advanced Battery Materials Research (BMR) Program (Battery500 Consortium) under Contract No. DE-EE0007764. Part of the work used the UCSD-MTI Battery Fabrication Facility and the UCSD-Arbin Battery Testing Facility. We acknowledge the Shenzhen CAPCHEM Technology Co. Ltd. for supplying the chemicals. The authors would like to thank Dr. Ich Tran for his help with the XPS experiments at the University of California, Irvine Materials Research Institute (IMRI) using instrumentation funded in part by the National Science Foundation Major Research Instrumentation Program under Grant No. CHE-1338173.

## Data Availability Statement

The raw/processed data required to reproduce these findings cannot be shared at this time as the data also forms part of an ongoing study.

## Appendix A. Supporting information

Supplementary data associated with this article can be found in the online version at doi:10.1016/j.ensm.2018.09.021.

## References

[1] W. Xu, J.L. Wang, F. Ding, X.L. Chen, E. Nasybutin, Y.H. Zhang, J.G. Zhang, Energ. Environ. Sci 7 (2014) 513–537.
[2] D. Lin, Y. Liu, Y. Cui, Nat. Nano 12 (2017) 194–206.
[3] X.B. Cheng, R. Zhang, C.Z. Zhao, Q. Zhang, Chem. Rev. 117 (2017) 10403–10473.
[4] M.D. Tikekar, S. Choudhury, Z. Tu, L.A. Archer, Nat. Energy 1 (2016) 16114.
[5] D. Aurbach, E. Zinigrad, Y. Cohen, H. Teller, Solid State Ion. 148 (2002) 405–416.
[6] H. Liu, X. Wang, H. Zhou, H.-D. Lim, X. Xing, Q. Yan, Y.S. Meng, P. Liu, ACS Appl. Energy Mater. 1 (2018) 1864–1869.
[7] H.D. Liu, H.Y. Zhou, B.S. Lee, X. Xing, M. Gonzalez, P. Liu, ACS Appl. Mater. Int. 9 (2017) 30635–30642.
[8] L. Liu, Y.X. Yin, J.Y. Li, S.H. Wang, Y.G. Guo, L.J. Wan, Adv. Mater. 30 (2018).
[9] X.L. Fan, L. Chen, X. Ji, T. Deng, S.Y. Hou, J. Chen, J. Zheng, F. Wang, J.J. Jiang, K. Xu, C.S. Wang, Chemistry 4 (2018) 174–185.
[10] H.D. Lim, H.K. Lim, X. Xing, B.S. Lee, H. Liu, C. Coaty, H. Kim, P. Liu, Adv. Mater. Interfaces 0 (2018) 1701328.
[11] N.W. Li, Y. Shi, Y.X. Yin, X.X. Zeng, J.Y. Li, C.J. Li, L.J. Wan, R. Wen, Y.G. Guo, Angew. Chem. Int. Ed. 57 (2018) 1505–1509.
[12] H.D. Lim, X.J. Yue, X. Xing, V. Petrova, M. Gonzalez, H.D. Liu, P. Liu, J Mater. Chem. A 6 (2018) 7370–7374.
[13] K. Xu, Chem. Rev. 114 (2014) 11503–11618.
[14] M.D. Radin, S. Hy, M. Sina, C.C. Fang, H.D. Liu, J. Vinckeviciute, M.H. Zhang, M.S. Whittingham, Y.S. Meng, A. Van der Ven, Adv. Energy Mater. 7 (2017).
[15] S. Hy, H.D. Liu, M.H. Zhang, D.N. Qian, B.J. Hwang, Y.S. Meng, Energ. Environ. Sci 9 (2016) 1931–1954.
[16] X. Ren, Y. Zhang, M.H. Engelhard, Q. Li, J.-G. Zhang, W. Xu, ACS Energy Lett. 3 (2018) 14–19.
[17] X. Ke, Y. Cheng, J. Liu, L. Liu, N. Wang, J. Liu, C. Zhi, Z. Shi, Z. Guo, ACS Appl. Mater. Int. 10 (2018) 13552–13561.
[18] D. Lin, Y. Liu, Z. Liang, H.-W. Lee, J. Sun, H. Wang, K. Yan, J. Xie, Y. Cui, Nat. Nanotechnol. 11 (2016) 626.
[19] C.P. Yang, Y.X. Yin, S.F. Zhang, N.W. Li, Y.G. Guo, Nat. Commun. 6 (2015).
[20] W.Y. Li, H.B. Yao, K. Yan, G.Y. Zheng, Z. Liang, Y.M. Chiang, Y. Cui, Nat. Commun. 6 (2015).
[21] B.D. Adams, E.V. Carino, J.G. Connell, K.S. Han, R.G. Cao, J.Z. Chen, J.M. Zheng, Q.Y. Li, K.T. Mueller, W.A. Henderson, J.G. Zhang, Nano Energy 40 (2017) 607–617.
[22] B.S. Lee, Z.H. Wu, V. Petrova, X. Xing, H.D. Lim, H.D. Liu, P. Liu, J Electrochem Soc. 165 (2018) A525–A533.
[23] H. Liu, H.D. Liu, S.H. Lapidus, Y.S. Meng, P.J. Chupas, K.W. Chapman, J Electrochem Soc. 164 (2017) A1802–A1811.
[24] H.D. Liu, H. Liu, I.D. Seymour, N. Chernova, K.M. Wiaderek, N.M. Trease, S. Hy, Y. Chen, K. An, M.H. Zhang, O.J. Borkiewicz, S.H. Lapidus, B. Qiu, Y.G. Xia, Z.P. Liu, P.J. Chupas, K.W. Chapman, M.S. Whittingham, C.P. Grey, Y.S. Meng, J Mater. Chem. A 6 (2018) 4189–4198.
[25] H.D. Liu, D.N. Qian, M.G. Verde, M.H. Zhang, L. Baggetto, K. An, Y. Chen, K.J. Carroll, D. Lau, M.F. Chi, G.M. Veith, Y.S. Meng, ACS Appl. Mater. Int. 7 (2015) 19189–19200.
[26] H.D. Liu, Y. Chen, S. Hy, K. An, S. Venkatachalam, D.N. Qian, M.H. Zhang, Y.S. Meng, Adv. Energy Mater. 6 (2016).
[27] J.J. Huang, H.D. Liu, N.X. Zhou, K. An, Y.S. Meng, J. Luo, ACS Appl. Mater. Int. 9 (2017) 36745–36754.
[28] Q.W. Shi, Y.R. Zhong, M. Wu, H.Z. Wang, H.L. Wang, Proc. Natl. Acad. Sci. USA 115 (2018) 5676–5680.